Jurnal Kejuruteraan 2 (1990) 213-223

THE FABRICATION AND EVALUATION OF ON-CHIP GAS PRESSURE SENSORS

Masuri bin Othman[1]

ABSTRAK

Di dalam kertas ini kita membincangkan pembikinan dan penilaian penderia tekanan gas yang berdasarkan kepada silikon. Penderia ini dibikinkan dengan menggunakan pembikinan litar terkamil piawai kecuali tahap punaran untuk membentuk rasuk julur. Rasuk julur adalah merupakan unsur utama dalam sistem penderia ini yang dipacu kepada titik resonan oleh perbezaan angkali pengembangan haba di antara silikon dan oksida. Pengesanan pada output dilakukan oleh kesan piezoresistif di dalam perintang polisikin yang ditakrifkan di atas lapisan oksida. Adalah didapati bahawa frekuensi resonan (f_R) berubah secara lelurus dengan tekanan gas dari 100 mmHg ke 500 mmHg. Oleh itu sistem penderia boleh digunakan sebagai penderia tekanan gas.

ABSTRACT

In this paper we describe the fabrication and evaluation of on-chip silicon-based gas pressure sensors. The sensor is fabricated using standard Integrated Circuit (IC) fabrication technology except the final etching to delineate cantilever beams. The beam which is the key element in the sensor system is driven to its resonant frequency by the difference in thermal expansion between silicon and oxide. The output detection is done by utilising the piezoresistive effect in a polysilicon resistor defined on top of the oxide layer. It is found that the resonant frequency (f_R) varies linearly with the gas pressure from 100 mmHg to about 500 mmH, thus it is possible for system to be used as a gas pressure sensor.

INTRODUCTION

Many new mechanical sensors fabricated by standard IC processing and microetching techniques have been produced recently [see for example Bassous et al, 1978]. The final microetching is required to define the shape of a sensor required for a particular application. Here we report on a realisation of a micromechanical cantilever beam and its use as a gas pressure sensor using the above method.

As shown in Figure 1, the sensor structure consists of a silicon beam (etched out from single crystal silicon) with overlying oxide layer. A polysilicon resistor is then defined on top of the oxide layer to be used as an exciter as well as a detector. A dc heating of the resistor will cause a differential thermal expansion between the polysilicon, oxide and silicon thus creating a non-zero bending moment which then triggers a bending of the beam. The detection of the bending is done by measuring the change in the polysilicon resistance since it is a piezoresitive material.

The possible use of the above structure as a gas pressure sensor can be established by monitoring a small shift in f_R in the sensing element induced by a varying gas pressure.

Analytical derivation of the relation between t_R and pressure p can be derived as follows:

ANALYSIS OF THE SENSITIVITY OF F_R WITH PRESSURE (CHRISTEN, 1983)

The mode shape and resonant frequency of a cantilever beam can be determined to a first order approximation by assuming that the beam is vibrating in a flexural mode. Using this assumption the free motion of the beam is given by the following equation.

$$EI \frac{\partial^4 y(x,t)}{\partial x^4} + \rho_c A \frac{\partial^2 y}{\partial t^2}(x,t) = 0 \qquad (1)$$

Where E and ρ_c are the Young's modulus and density of the material and A and I are the surface area and moment of inertia of the cross-section of the beam. By using separation of space and time variables for the mode shape we have:

$$\frac{d^4 y}{dx^4} - n^4 y = 0 \qquad (2a)$$

where

$$n^4 = \frac{\rho_c A}{EI} \omega^2 \qquad (2b)$$

and the eigenfrequencies are given by:

$$\omega_n = \frac{\alpha_n^2}{L^2} - \frac{EI}{\rho_c A} \qquad (3)$$

Where the α_n are modal constants given by the boundary condition:

$$\cos \alpha_n L + \cosh \alpha_n L + 1 = 0 \qquad (4)$$

However when a solid body undergoes harmonic oscillations of small amplitudes in a fluid medium (gas or liquid), it tends to induce particle motion in the fluid which gives rise to energy loss and additional inertia. Then the equation of motion in (1) becomes:

$$EI \frac{\partial^4 y}{\partial x^4}(x,t) + \xi \frac{\partial Y}{\partial t}(x,y) + (\rho A + \mu) \frac{\partial^2 y}{\partial t^2}(x,t) = 0 \qquad (5)$$

where ξ and μ are the damping parameter and added mass due to inertia respectively.

From above, one gets the mode shape as below:

$$\frac{d^4 y}{dx^4} - z^{*4} y = 0 \qquad (6a)$$

Where

$$Z^{*4} = \frac{(\rho_c A + \mu)}{(EI)} \omega^2 \left[1 - \frac{\xi}{(\rho_c A + \mu)} I \right] \qquad (6b)$$

$$= n^4 (1 - \delta I)$$

where

$$n^4 = \frac{(\rho_c A + \mu)}{(EI)} \omega^2 \text{ and } \delta = \frac{\xi}{(\rho_c A + \mu)}$$

The mode shape in equation 6(b) is suitable for beam bending in any medium which has any values of damping parameters. However if the medium is gas, then the effect of damping can be neglected. Using this assumption, the expression for f_R takes the form of:

$$f_n = \frac{1}{2\pi} \frac{\alpha_m^2}{L^2} \frac{EI}{(\rho_c A + \mu)}^{1/2} \tag{7}$$

or

$$f_n \approx \frac{1}{2\pi} \frac{\alpha_n^2}{L^2} \frac{EI}{(\rho_c A)}^{1/2} \frac{1}{1 + (\mu/\rho_c A)}^{1/2} \tag{8}$$

Since the damping is small, equation (8) can now be written as:

$$f_n = f_{on} \left(1 - \frac{1}{2} \frac{\mu}{\rho_c A}\right) \tag{9}$$

Where f_{on} are the resonant frequencies of the cantilever beam in vacuum. Blake, (1974) has shown that the added mass approximately equals to $2m_o$, where m_o is the mass of the gas per unit length given by:

$$m_o = \pi \rho_g w^2/4 \tag{10}$$

Where ρ_g and w are the gas density and beam's width respectively. Inserting equation (10) into (a) and using relation

$$\rho_g = \left(\frac{M}{RT}\right)P, \text{ we have}$$

$$\frac{df}{dp} = \frac{\pi}{4}\left(\frac{W}{t}\right)\left(\frac{f_o}{\rho_g}\right)\left(\frac{M}{RT}\right) \qquad (11)$$

Where M, ρ, R and T are the molecular weight, pressure, gas constant and temperature respectively.

EXPERIMENTAL SET–UP

Figure (2) shows a circuit arrangement used to detect the f_R of a cantilever beam. The sample is located in an aluminium pot so that the inside pressure can be varied. Since for our device the same resistor is used to excite and detect the beam, a bridge configuration as shown in Figure (2) is required.

Initially the bridge is balanced until no output signal is observed on the scope. The value of f_R is determined from a spectrum analyzer by slowly tuning a frequency meter until a sudden increase in the output is observed. A sudden increase in the amplitude occurs when the input frequency equals to the resonant frequency of the beam. The same procedure is repeated for other values of pressure. In this experiment, the air pressure is measured although other types of gases are possible.

RESULTS AND DISCUSSION.

Figure (3) shows the output response obtained from the spectrum analyzer. The beam is about 60μm length, 20μm thick and 18μm wide. As expected the output signal is maximum when the input drive frequency equals to the resonant frequency of the beam. A sudden decrease in amplitude is also observed for other frequencies differs from f_R. It can be seen that for this particular beam its f_R is about 646.8 KHz and has a bandwidth of about 4000 Hz.

Figure (4) shows the measured variation of f_R and (1/Q) with the change in air pressure. It can be seen that the response of the system to the air pressure is linear in the region considered with the sensitivity of about 5 ppm/mmHg. The value of Q at lower (<120 mmHg) and higher pressure (from mmHg to 760 mmHg) are not included in the figure. This is because in the former case a reasonable pressure control is not achieved which required our experimental set up to be upgraded. While the operation at higher pressure gives poor output signal from the bridge. Consequently the value of Q observed from the frequency response curve is not accurate. For this reason, it is suggested that in future, a self-

oscillating resonator which incorporates positive feedback is used. The beam is also observed to resonate at atmospheric pressure with Q = 300 approximately.

The value of f_o in equation (11) can be obtained from the graph by interpolating the frequency line to zero pressure axis. This enables us to estimate the sensitivity of the sensor which is about 4.5 ppm/mmHg. Thus a reasonable agreement is obtained between the measured and calculated values.

It is abvious that the sensor sensitivity is relatively small as compred to the one reported by Christen [1983]. One of the techniques to improve the sensor sensitivitty is to reduce the f_R given in (11). The sensitivity can be improve further by increasing the width of the beam. A paddle shapped cantilever is also expected to show a greater sensitivity.

CONCLUSION

From the above discussion it can be seen that the micromechanical resonator can be used to measure the air pressure. For our device the sensitivity obtained is about 5 ppm/mmHg which is in reasonable agreement with the predicted value in equation (11).

Notation

A	Area
E	Young's modulus
f_R	resonant frequency
f_{on}	resonant frequencies in vacuum
I	moment of inertia
L_M	length of the beam
M_o	Molecular weight
μ	added mass
n	mode number
P	Pressure
R	gas constant

T	Temperature in Kelvin
w	width of the beam
x	displacement
y	displacement
ρ_c	density,
ρ_g	gas density
ξ	damping parameter
ω	eigen frequency

REFERENCE

Bassous, E., Taub, H.H., and Kuhn, L. (1977). Ink jet printing nozzle silicon. App. Phys. Lett., Vol. 31, P. 135.

Blake, W.T. (1974). The Radiation free-free beams in air and water. J. Sound Vibration, 33, 427-450.

Christen, M (1983). Air and gas damping of Quartz tuning forks, Sensor and Actuators, 4, 555-564.

Figure Caption

Figure 1: The structure of a mechanical reconator.

Figure 2: Bridge technique of detecting resonance.

Figure 3: Typical frequency response of a resonator.

Figure 4: The dependence of f_R and Q-factor with gas pressure.

1 Jabatan Kejuruteraan Elektrik, Elektronik & Sistem
Universiti Kebangsaan Malaysia.

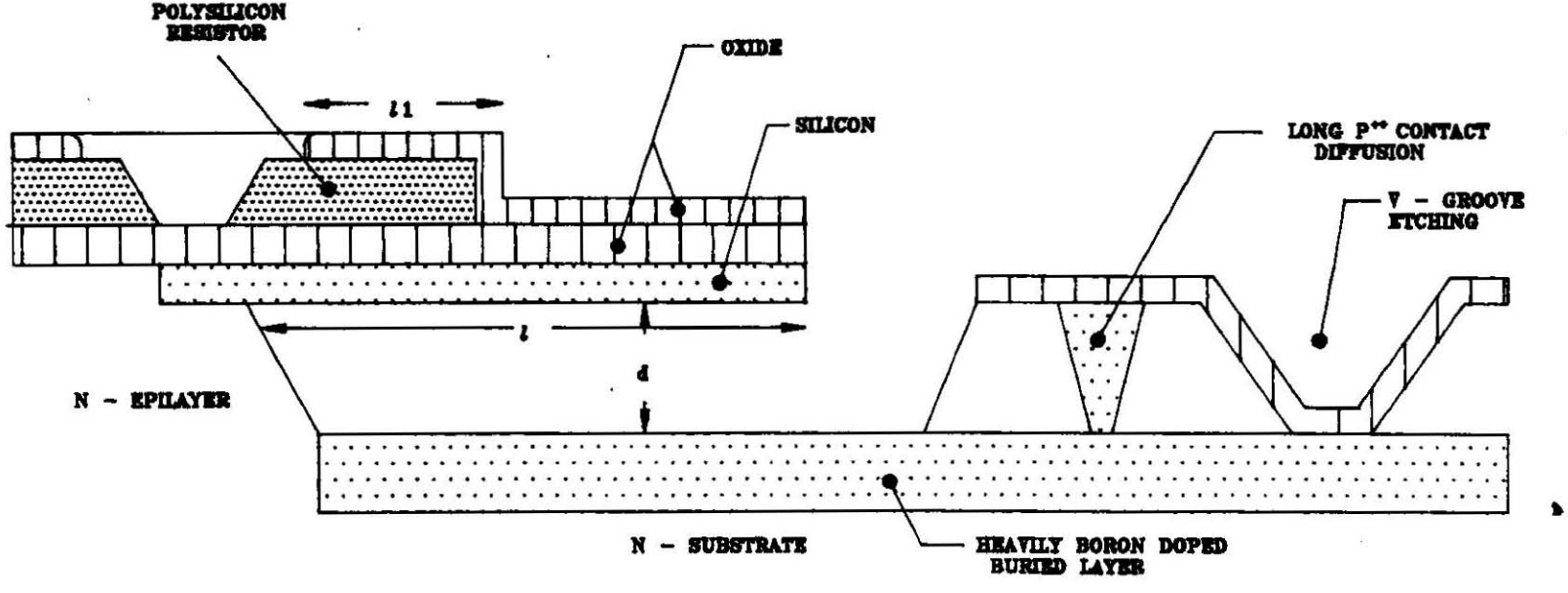

Figure 1 : Structure of a Mechanical Resonator

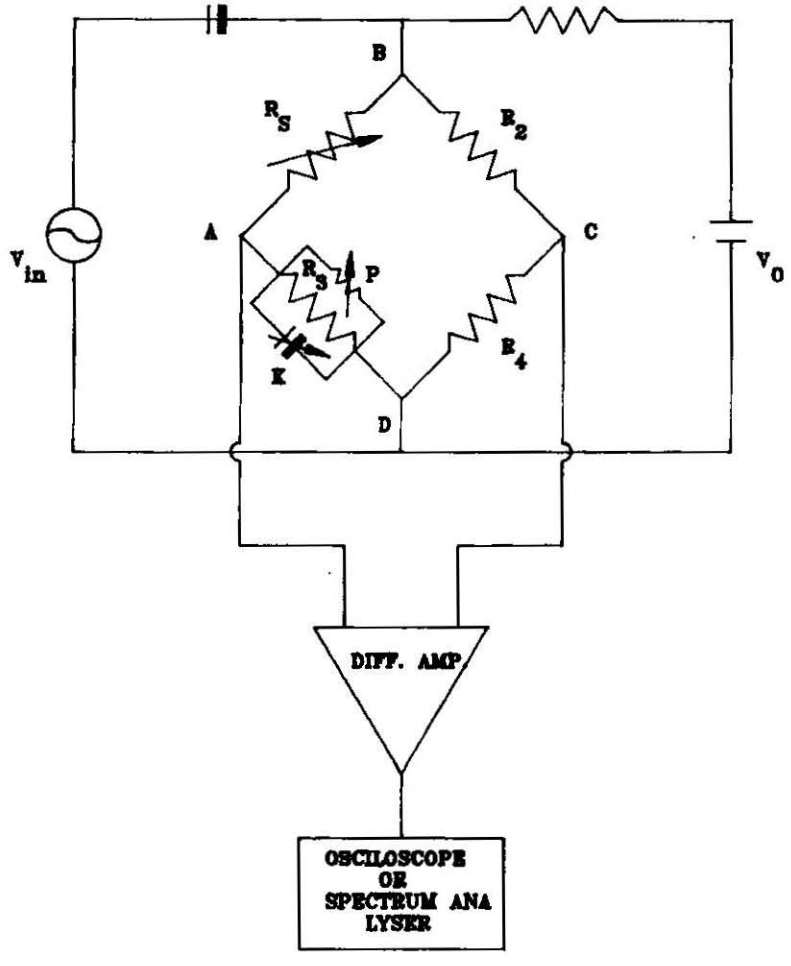

Figure 2 : Bridge Technique of Detecting Resonance

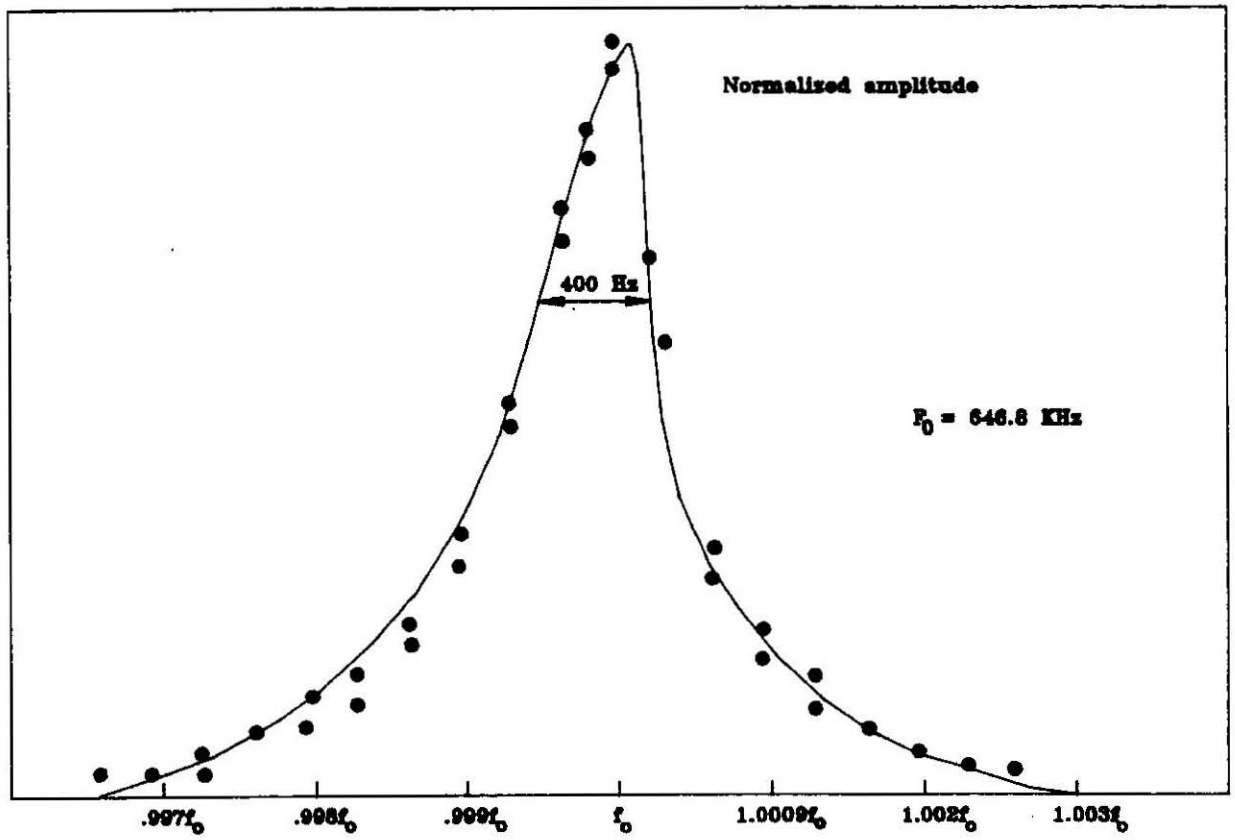

Figure 3 : Shows the Typical Frequency Response of a Resonator

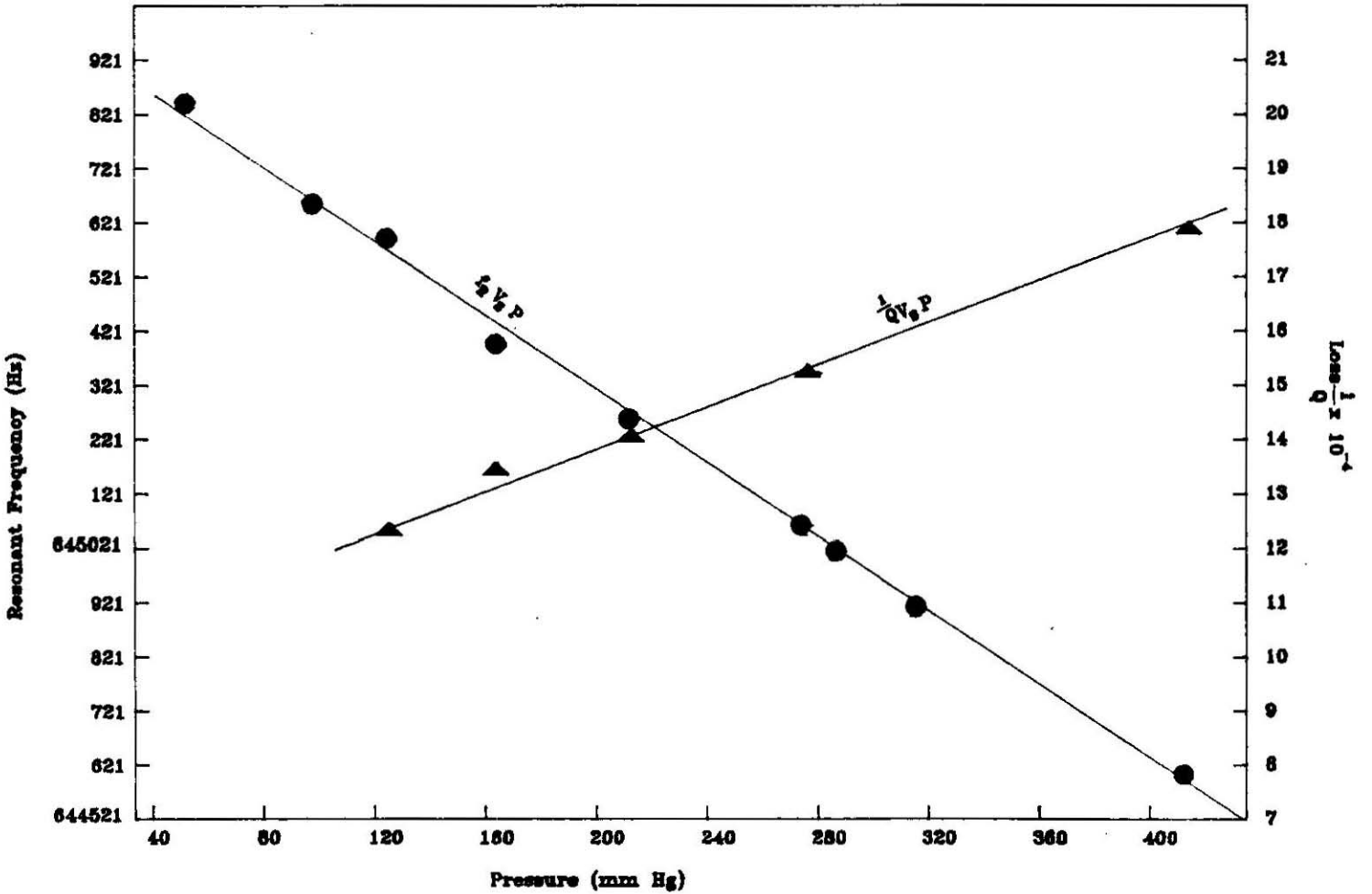

Figure 4 : The Dependence of Resonant Frequency and Q-Factor With Gas Pressure